Full-sky interferometry

Simulating full-sky interferometric observations with wavelets

Jason McEwen
http://www.jasonmcewen.org/

BASP research node

Institute of Electrical Engineering,
Ecole Polytechnique Fédérale de Lausanne (EPFL), Switzerland

Cavendish Astrophysics Seminar :: Cambridge :: September 2010

Outline

Outline

1. Full-sky interferometry formulation
   - Mathematical preliminaries
   - Coordinate systems
   - Visibility representation
   - Image reconstruction

2. Wavelets on the sphere
   - Why wavelets?
   - Haar wavelets on the sphere

3. Full-sky interferometry formulation revisited with wavelets
   - SHW visibility representation
   - Fast wavelet algorithms

4. Simulations
   - Low-resolution comparison
   - High-resolution illustration

5. Summary

Preliminaries: spherical harmonics

- A square integrable function on the sphere $F \in \mathrm{L}^2(\mathrm{S}^2,\ \mathrm{d}\Omega)$ may be represented by the spherical harmonic expansion

$$F(\hat{\mathbf{s}}) = \sum_{\ell=0}^{\infty} \sum_{m=-\ell}^{\ell} F_{\ell m} Y_{\ell m}(\hat{\mathbf{s}}) \ .$$

- The spherical harmonic coefficients are given by the usual projection onto the spherical harmonic basis functions:

$$F_{\ell m} = \int_{\mathrm{S}^2} F(\hat{\mathbf{s}})\ Y_{\ell m}^{*}(\hat{\mathbf{s}})\ \mathrm{d}\Omega(\hat{\mathbf{s}})\ ,$$

where $\mathrm{d}\Omega(\hat{\mathbf{s}}) = \sin\theta\,\mathrm{d}\theta\,\mathrm{d}\varphi$ is the usual rotation invariant measure on the sphere and $\hat{\mathbf{s}} = (\theta, \varphi) \in \mathrm{S}^2$ denote spherical coordinates with colatitude $\theta \in [0, \pi]$ and longitude $\varphi \in [0, 2\pi)$.

- Useful properties and relations
  - Orthogonality

$$\int_{\mathrm{S}^2} Y_{\ell m}(\hat{\mathbf{s}})\ Y_{\ell' m'}^{*}(\hat{\mathbf{s}})\ \mathrm{d}\Omega(\hat{\mathbf{s}}) = \delta_{\ell\ell'}\delta_{mm'}$$

  - Addition theorem

$$\sum_{m=-\ell}^{\ell} Y_{\ell m}(\hat{\mathbf{s}}) Y_{\ell m}^{*}(\hat{\mathbf{s}}') = \frac{2\ell+1}{4\pi} P_\ell(\hat{\mathbf{s}} \cdot \hat{\mathbf{s}}')$$

  - Jacobi-Anger expansion

$$\mathrm{e}^{\mathrm{i}\boldsymbol{x}\cdot\boldsymbol{y}} = \sum_{\ell=0}^{\infty} (2\ell+1)\mathrm{i}^\ell j_\ell(\|\boldsymbol{x}\|\|\boldsymbol{y}\|) P_\ell(\hat{\boldsymbol{x}} \cdot \hat{\boldsymbol{y}})$$

Preliminaries: spherical harmonics

- A square integrable function on the sphere $F \in \mathrm{L}^2(\mathrm{S}^2, \mathrm{d}\Omega)$ may be represented by the spherical harmonic expansion

$$F(\hat{\boldsymbol{s}}) = \sum_{\ell=0}^{\infty} \sum_{m=-\ell}^{\ell} F_{\ell m} Y_{\ell m}(\hat{\boldsymbol{s}}) \ .$$

- The spherical harmonic coefficients are given by the usual projection onto the spherical harmonic basis functions:

$$F_{\ell m} = \int_{\mathrm{S}^2} F(\hat{\boldsymbol{s}}) \ Y_{\ell m}^*(\hat{\boldsymbol{s}}) \ \mathrm{d}\Omega(\hat{\boldsymbol{s}}) \ ,$$

  where $\mathrm{d}\Omega(\hat{\boldsymbol{s}}) = \sin\theta \, \mathrm{d}\theta \, \mathrm{d}\varphi$ is the usual rotation invariant measure on the sphere and $\hat{\boldsymbol{s}} = (\theta, \varphi) \in \mathrm{S}^2$ denote spherical coordinates with colatitude $\theta \in [0, \pi]$ and longitude $\varphi \in [0, 2\pi)$.

- Useful properties and relations
  - Orthogonality

$$\int_{\mathrm{S}^2} Y_{\ell m}(\hat{\boldsymbol{s}}) \ Y_{\ell' m'}^*(\hat{\boldsymbol{s}}) \ \mathrm{d}\Omega(\hat{\boldsymbol{s}}) = \delta_{\ell\ell'} \delta_{mm'}$$

  - Addition theorem

$$\sum_{m=-\ell}^{\ell} Y_{\ell m}(\hat{\boldsymbol{s}}) Y_{\ell m}^*(\hat{\boldsymbol{s}}') = \frac{2\ell + 1}{4\pi} P_\ell(\hat{\boldsymbol{s}} \cdot \hat{\boldsymbol{s}}')$$

  - Jacobi-Anger expansion

$$\mathrm{e}^{\mathrm{i}\boldsymbol{x}\cdot\boldsymbol{y}} = \sum_{\ell=0}^{\infty} (2\ell + 1) \mathrm{i}^\ell j_\ell(\|\boldsymbol{x}\| \|\boldsymbol{y}\|) P_\ell(\hat{\boldsymbol{x}} \cdot \hat{\boldsymbol{y}})$$

Preliminaries: rotations

- Rotations on the sphere $\mathcal{R}$ characterised by the the rotation group $\mathrm{SO}(3)$, which we parameterise in terms of the three Euler angles $\rho = (\alpha, \beta, \gamma) \in \mathrm{SO}(3)$, where $\alpha \in [0, 2\pi)$, $\beta \in [0, \pi]$ and $\gamma \in [0, 2\pi)$.
- Rotation of coordinate vector performed by multiplication with 3×3 rotation matrix

$$\mathbf{R}(\rho) = \mathbf{R}_z(\alpha)\mathbf{R}_y(\beta)\mathbf{R}_z(\gamma) \ ,$$

where $\mathbf{R}_z(\vartheta)$ and $\mathbf{R}_y(\vartheta)$ are rotation matrices representing rotations by ϑ about the z and y axis respectively (adopt zyz Euler convention).

- Rotation of function on the sphere defined by

$$\big(\mathcal{R}(\rho)F\big)(\hat{\mathbf{s}}) = F\big(\mathbf{R}^{-1}(\rho)\hat{\mathbf{s}}\big) \ .$$

- Rotation of function on sphere may be performed more generally (*i.e.* pixelisation independent) and accurately through harmonic space representation. Harmonic coefficients of a rotated function are related to the coefficients of the original function by

$$\big(\mathcal{R}(\rho)F\big)_{\ell m} = \sum_{n=-\ell}^{\ell} D^{\ell}_{mn}(\rho)\, F_{\ell n} \ ,$$

where the Wigner D-functions $D^{\ell}_{mn}(\rho)$ provide the irreducible unitary representation of the rotation group $\mathrm{SO}(3)$.

Preliminaries: rotations

- Rotations on the sphere $\mathcal{R}$ characterised by the the rotation group $\mathrm{SO}(3)$, which we parameterise in terms of the three Euler angles $\rho = (\alpha, \beta, \gamma) \in \mathrm{SO}(3)$, where $\alpha \in [0, 2\pi)$, $\beta \in [0, \pi]$ and $\gamma \in [0, 2\pi)$.
- Rotation of coordinate vector performed by multiplication with 3×3 rotation matrix

$$\mathbf{R}(\rho) = \mathbf{R}_z(\alpha)\mathbf{R}_y(\beta)\mathbf{R}_z(\gamma) \ ,$$

  where $\mathbf{R}_z(\vartheta)$ and $\mathbf{R}_y(\vartheta)$ are rotation matrices representing rotations by ϑ about the z and y axis respectively (adopt zyz Euler convention).
- Rotation of function on the sphere defined by

$$\big(\mathcal{R}(\rho)F\big)(\hat{\mathbf{s}}) = F\big(\mathbf{R}^{-1}(\rho)\hat{\mathbf{s}}\big) \ .$$

- Rotation of function on sphere may be performed more generally (*i.e.* pixelisation independent) and accurately through harmonic space representation. Harmonic coefficients of a rotated function are related to the coefficients of the original function by

$$\big(\mathcal{R}(\rho)F\big)_{\ell m} = \sum_{n=-\ell}^{\ell} D^{\ell}_{mn}(\rho)\, F_{\ell n} \ ,$$

  where the Wigner D-functions $D^{\ell}_{mn}(\rho)$ provide the irreducible unitary representation of the rotation group $\mathrm{SO}(3)$.

Coordinate systems

- The complex visibility measured by an interferometer is given by the coordinate free definition

$$\mathcal{V}(\boldsymbol{u}) = \int_{\mathbb{S}^2} A(\boldsymbol{\sigma}) I(\boldsymbol{\sigma}) \mathrm{e}^{-\mathrm{i}2\pi \boldsymbol{u}\cdot\boldsymbol{\sigma}} \, \mathrm{d}\Omega \, .$$

- In this coordinate free definition, $\boldsymbol{\sigma}$ is the representation of $\hat{\boldsymbol{s}}$ in a coordinate system centred on $\hat{\boldsymbol{s}}_0$. The translation $\boldsymbol{\sigma} = \hat{\boldsymbol{s}} - \hat{\boldsymbol{s}}_0$ represents the transformation between the global coordinate frame of $\hat{\boldsymbol{s}}$ and the local coordinate frame of $\boldsymbol{\sigma}$.
- In general, one can transform vectors between global coordinates and local coordinates relative to $\hat{s}_0$, through a rotation by $\hat{s}_0$.
- The rotation $\mathcal{R}_0 \equiv \mathcal{R}(\varphi_0, \theta_0, 0)$, where (θ_0, φ_0) are the spherical coordinates of $\hat{s}_0$, transforms the local coordinate frame relative to $\hat{s}_0$ to the global coordinate frame of the celestial sky.
- Local coordinates are related to global coordinates by $\hat{s}^{\mathrm{l}} = \mathbf{R}_0^{-1} \hat{s}^{\mathrm{n}}$, where $\mathbf{R}_0$ is the 3×3 rotation matrix corresponding to the rotation $\mathcal{R}_0$.

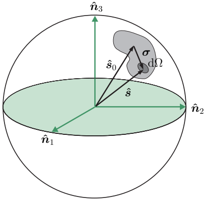

Figure: Geometry of observation of extended source.

Coordinate systems

- The complex visibility measured by an interferometer is given by the coordinate free definition

$$\mathcal{V}(\boldsymbol{u}) = \int_{\mathbb{S}^2} A(\boldsymbol{\sigma}) I(\boldsymbol{\sigma}) \mathrm{e}^{-\mathrm{i}2\pi \boldsymbol{u}\cdot\boldsymbol{\sigma}} \, \mathrm{d}\Omega \, .$$

- In this coordinate free definition, $\boldsymbol{\sigma}$ is the representation of $\hat{\boldsymbol{s}}$ in a coordinate system centred on $\hat{\boldsymbol{s}}_0$. The translation $\boldsymbol{\sigma} = \hat{\boldsymbol{s}} - \hat{\boldsymbol{s}}_0$ represents the transformation between the global coordinate frame of $\hat{\boldsymbol{s}}$ and the local coordinate frame of $\boldsymbol{\sigma}$.
- In general, one can transform vectors between global coordinates and local coordinates relative to $\hat{\boldsymbol{s}}_0$, through a rotation by $\hat{\boldsymbol{s}}_0$.
- The rotation $\mathcal{R}_0 \equiv \mathcal{R}(\varphi_0, \theta_0, 0)$, where (θ_0, φ_0) are the spherical coordinates of $\hat{\boldsymbol{s}}_0$, transforms the local coordinate frame relative to $\hat{\boldsymbol{s}}_0$ to the global coordinate frame of the celestial sky.
- Local coordinates are related to global coordinates by $\hat{\boldsymbol{s}}^{\mathrm{l}} = \mathbf{R}_0^{-1} \hat{\boldsymbol{s}}^{\mathrm{n}}$, where $\mathbf{R}_0$ is the 3×3 rotation matrix corresponding to the rotation $\mathcal{R}_0$.

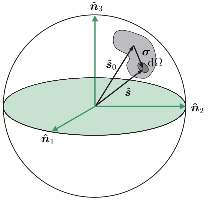

Figure: Geometry of observation of extended source.

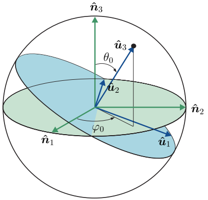

Figure: Rotation $\mathcal{R}_0$ mapping global coordinates of the celestial sky to local coordinates.

Coordinate systems

- Returning to the visibility function, we may now represent each function in its most natural coordinate system:
  - The beam function is most naturally represented in local coordinates relative to the pointing direction $\hat{s}_0^{\mathrm{n}}$ and is denoted by $A^{\mathrm{l}}(\hat{\boldsymbol{s}}^{\mathrm{l}})$.
  - The source intensity function is most naturally represented in global coordinates and is denoted by $I^{\mathrm{n}}(\hat{\boldsymbol{s}}^{\mathrm{n}})$.

- We may convert function F^{n} in global coordinates to a corresponding function F^{l} in local coordinates through the rotation $\mathcal{R}_0$:

$$F^{\mathrm{n}}(\hat{\boldsymbol{s}}^{\mathrm{n}}) = F^{\mathrm{n}}(\mathbf{R}_0\hat{\boldsymbol{s}}^{\mathrm{l}}) = (\mathcal{R}_0^{-1}F^{\mathrm{n}})(\hat{\boldsymbol{s}}^{\mathrm{l}}) = F^{\mathrm{l}}(\hat{\boldsymbol{s}}^{\mathrm{l}}) , \quad \textit{i.e. } F^{\mathrm{l}} = \mathcal{R}_0^{-1}F^{\mathrm{n}} .$$

- The visibility integral may then be written

$$\mathcal{V}(\boldsymbol{u}) = \int_{\mathrm{S}^2} A^{\mathrm{l}}(\hat{\boldsymbol{s}}^{\mathrm{l}}) I^{\mathrm{n}}(\hat{\boldsymbol{s}}^{\mathrm{n}}) \mathrm{e}^{-\mathrm{i}2\pi\boldsymbol{u}\cdot\hat{\boldsymbol{s}}^{\mathrm{l}}} \, \mathrm{d}\Omega(\hat{\boldsymbol{s}}^{\mathrm{l}}) ,$$

or in local coordinates

$$\mathcal{V}(\boldsymbol{u}) = \int_{\mathrm{S}^2} A^{\mathrm{l}}(\hat{\boldsymbol{s}}^{\mathrm{l}}) (\mathcal{R}_0^{-1} I^{\mathrm{n}})(\hat{\boldsymbol{s}}^{\mathrm{l}}) \mathrm{e}^{-\mathrm{i}2\pi\boldsymbol{u}\cdot\hat{\boldsymbol{s}}^{\mathrm{l}}} \, \mathrm{d}\Omega(\hat{\boldsymbol{s}}^{\mathrm{l}})$$

$$= \int_{\mathrm{S}^2} A^{\mathrm{l}}(\hat{\boldsymbol{s}}^{\mathrm{l}}) I^{\mathrm{l}}(\hat{\boldsymbol{s}}^{\mathrm{l}}) \mathrm{e}^{-\mathrm{i}2\pi\boldsymbol{u}\cdot\hat{\boldsymbol{s}}^{\mathrm{l}}} \, \mathrm{d}\Omega(\hat{\boldsymbol{s}}^{\mathrm{l}}) .$$

Coordinate systems

- Returning to the visibility function, we may now represent each function in its most natural coordinate system:
  - The beam function is most naturally represented in local coordinates relative to the pointing direction $\hat{s}_0^{\mathrm{n}}$ and is denoted by $A^{\mathrm{l}}(\hat{\boldsymbol{s}}^{\mathrm{l}})$.
  - The source intensity function is most naturally represented in global coordinates and is denoted by $I^{\mathrm{n}}(\hat{\boldsymbol{s}}^{\mathrm{n}})$.
- We may convert function F^{n} in global coordinates to a corresponding function F^{l} in local coordinates through the rotation $\mathcal{R}_0$:

$$F^{\mathrm{n}}(\hat{\boldsymbol{s}}^{\mathrm{n}}) = F^{\mathrm{n}}(\mathbf{R}_0\hat{\boldsymbol{s}}^{\mathrm{l}}) = (\mathcal{R}_0^{-1}F^{\mathrm{n}})(\hat{\boldsymbol{s}}^{\mathrm{l}}) = F^{\mathrm{l}}(\hat{\boldsymbol{s}}^{\mathrm{l}}) \ , \quad \textit{i.e.}\ F^{\mathrm{l}} = \mathcal{R}_0^{-1}F^{\mathrm{n}} \ .$$

- The visibility integral may then be written

$$\mathcal{V}(\boldsymbol{u}) = \int_{\mathrm{S}^2} A^{\mathrm{l}}(\hat{\boldsymbol{s}}^{\mathrm{l}}) I^{\mathrm{n}}(\hat{\boldsymbol{s}}^{\mathrm{n}}) \mathrm{e}^{-\mathrm{i}2\pi\boldsymbol{u}\cdot\hat{\boldsymbol{s}}^{\mathrm{l}}} \, \mathrm{d}\Omega(\hat{\boldsymbol{s}}^{\mathrm{l}}) \ ,$$

  or in local coordinates

$$\begin{aligned}\mathcal{V}(\boldsymbol{u}) &= \int_{\mathrm{S}^2} A^{\mathrm{l}}(\hat{\boldsymbol{s}}^{\mathrm{l}}) (\mathcal{R}_0^{-1}I^{\mathrm{n}})(\hat{\boldsymbol{s}}^{\mathrm{l}}) \mathrm{e}^{-\mathrm{i}2\pi\boldsymbol{u}\cdot\hat{\boldsymbol{s}}^{\mathrm{l}}} \, \mathrm{d}\Omega(\hat{\boldsymbol{s}}^{\mathrm{l}}) \\ &= \int_{\mathrm{S}^2} A^{\mathrm{l}}(\hat{\boldsymbol{s}}^{\mathrm{l}}) I^{\mathrm{l}}(\hat{\boldsymbol{s}}^{\mathrm{l}}) \mathrm{e}^{-\mathrm{i}2\pi\boldsymbol{u}\cdot\hat{\boldsymbol{s}}^{\mathrm{l}}} \, \mathrm{d}\Omega(\hat{\boldsymbol{s}}^{\mathrm{l}}) \ .\end{aligned}$$

Visibility representation

- Substituting the harmonic expansion of the beam-modulated source intensity function $\left(A^{\mathrm{l}} \cdot I^{\mathrm{l}}\right)(\hat{\boldsymbol{s}}^{\mathrm{l}}) = A^{\mathrm{l}}(\hat{\boldsymbol{s}}^{\mathrm{l}}) I^{\mathrm{l}}(\hat{\boldsymbol{s}}^{\mathrm{l}})$, visibility integral becomes

$$\mathcal{V}(\boldsymbol{u}) = \sum_{\ell m} \left(A^{\mathrm{l}} \cdot I^{\mathrm{l}}\right)_{\ell m} \int_{\mathrm{S}^2} \mathrm{e}^{-\mathrm{i}2\pi \boldsymbol{u} \cdot \hat{\boldsymbol{s}}^{\mathrm{l}}} Y_{\ell m}(\hat{\boldsymbol{s}}^{\mathrm{l}}) \, \mathrm{d}\Omega(\hat{\boldsymbol{s}}^{\mathrm{l}}) \, .$$

- Using the addition theorem for spherical harmonics, the Jacobi-Anger expansion and the orthogonality of the spherical harmonics the above integral can be evaluated analytically:

$$\int_{\mathrm{S}^2} \mathrm{e}^{-\mathrm{i}2\pi \boldsymbol{u} \cdot \hat{\boldsymbol{s}}^{\mathrm{l}}} Y_{\ell m}(\hat{\boldsymbol{s}}^{\mathrm{l}}) \, \mathrm{d}\Omega(\hat{\boldsymbol{s}}^{\mathrm{l}}) = 4\pi (-\mathrm{i})^{\ell} j_{\ell}(2\pi \|\boldsymbol{u}\|) Y_{\ell m}(\hat{\boldsymbol{u}}) \, .$$

- The harmonic representation of the full-sky visibility function then reads:

Harmonic representation of visibility

$$\mathcal{V}(\boldsymbol{u}) = 4\pi \sum_{\ell m} (-\mathrm{i})^{\ell} j_{\ell}(2\pi \|\boldsymbol{u}\|) Y_{\ell m}(\hat{\boldsymbol{u}}) \left(A^{\mathrm{l}} \cdot I^{\mathrm{l}}\right)_{\ell m}$$

Visibility representation

- Substituting the harmonic expansion of the beam-modulated source intensity function $(A^{\mathrm{l}} \cdot I^{\mathrm{l}})(\hat{\boldsymbol{s}}^{\mathrm{l}}) = A^{\mathrm{l}}(\hat{\boldsymbol{s}}^{\mathrm{l}}) I^{\mathrm{l}}(\hat{\boldsymbol{s}}^{\mathrm{l}})$, visibility integral becomes

$$\mathcal{V}(\boldsymbol{u}) = \sum_{\ell m} \left(A^{\mathrm{l}} \cdot I^{\mathrm{l}}\right)_{\ell m} \int_{\mathrm{S}^2} \mathrm{e}^{-\mathrm{i}2\pi \boldsymbol{u} \cdot \hat{\boldsymbol{s}}^{\mathrm{l}}} Y_{\ell m}(\hat{\boldsymbol{s}}^{\mathrm{l}}) \, \mathrm{d}\Omega(\hat{\boldsymbol{s}}^{\mathrm{l}}) \; .$$

- Using the addition theorem for spherical harmonics, the Jacobi-Anger expansion and the orthogonality of the spherical harmonics the above integral can be evaluated analytically:

$$\int_{\mathrm{S}^2} \mathrm{e}^{-\mathrm{i}2\pi \boldsymbol{u} \cdot \hat{\boldsymbol{s}}^{\mathrm{l}}} Y_{\ell m}(\hat{\boldsymbol{s}}^{\mathrm{l}}) \, \mathrm{d}\Omega(\hat{\boldsymbol{s}}^{\mathrm{l}}) = 4\pi (-\mathrm{i})^{\ell} j_{\ell}(2\pi \|\boldsymbol{u}\|) Y_{\ell m}(\hat{\boldsymbol{u}}) \; .$$

- The harmonic representation of the full-sky visibility function then reads:

Harmonic representation of visibility

$$\mathcal{V}(\boldsymbol{u}) = 4\pi \sum_{\ell m} (-\mathrm{i})^{\ell} j_{\ell}(2\pi \|\boldsymbol{u}\|) Y_{\ell m}(\hat{\boldsymbol{u}}) \left(A^{\mathrm{l}} \cdot I^{\mathrm{l}}\right)_{\ell m}$$

Visibility representation

- Substituting the harmonic expansion of the beam-modulated source intensity function $\left(A^{\mathrm{l}} \cdot I^{\mathrm{l}}\right)(\hat{\boldsymbol{s}}^{\mathrm{l}}) = A^{\mathrm{l}}(\hat{\boldsymbol{s}}^{\mathrm{l}}) I^{\mathrm{l}}(\hat{\boldsymbol{s}}^{\mathrm{l}})$, visibility integral becomes

$$\mathcal{V}(\boldsymbol{u}) = \sum_{\ell m} \left(A^{\mathrm{l}} \cdot I^{\mathrm{l}}\right)_{\ell m} \int_{\mathrm{S}^2} \mathrm{e}^{-\mathrm{i}2\pi \boldsymbol{u} \cdot \hat{\boldsymbol{s}}^{\mathrm{l}}} Y_{\ell m}(\hat{\boldsymbol{s}}^{\mathrm{l}}) \, \mathrm{d}\Omega(\hat{\boldsymbol{s}}^{\mathrm{l}}) \; .$$

- Using the addition theorem for spherical harmonics, the Jacobi-Anger expansion and the orthogonality of the spherical harmonics the above integral can be evaluated analytically:

$$\int_{\mathrm{S}^2} \mathrm{e}^{-\mathrm{i}2\pi \boldsymbol{u} \cdot \hat{\boldsymbol{s}}^{\mathrm{l}}} Y_{\ell m}(\hat{\boldsymbol{s}}^{\mathrm{l}}) \, \mathrm{d}\Omega(\hat{\boldsymbol{s}}^{\mathrm{l}}) = 4\pi (-\mathrm{i})^{\ell} j_{\ell}(2\pi \|\boldsymbol{u}\|) Y_{\ell m}(\hat{\boldsymbol{u}}) \; .$$

- The harmonic representation of the full-sky visibility function then reads:

Harmonic representation of visibility

$$\mathcal{V}(\boldsymbol{u}) = 4\pi \sum_{\ell m} (-\mathrm{i})^{\ell} j_{\ell}(2\pi \|\boldsymbol{u}\|) Y_{\ell m}(\hat{\boldsymbol{u}}) \left(A^{\mathrm{l}} \cdot I^{\mathrm{l}}\right)_{\ell m}$$

Image reconstruction

- Full-sky image reconstruction is possible in theory:

$$\int_{S^2} \mathcal{V}(\boldsymbol{u}) Y_{\ell m}^*(\hat{\boldsymbol{u}}) \, \mathrm{d}\Omega(\hat{\boldsymbol{u}}) = 4\pi(-\mathrm{i})^\ell j_\ell(2\pi\|\boldsymbol{u}\|) \left(A^1 \cdot I^1\right)_{\ell m} .$$

- But not in practise since would require full sampling of the visibility function in $\mathbb{R}^3$.
- Instead use:
  - Standard Fourier transform approach for small patches.
  - w-projection (Cornwell *et al.* [3]) or faceting (Cornwell & Perley [4]) approaches for wide fields of view.
- We consider only the forward problem of simulating visibilities in the full-sky setting and do not consider the reverse problem of image reconstruction any further.

Image reconstruction

- Full-sky image reconstruction is possible in theory:

$$\int_{S^2} \mathcal{V}(\boldsymbol{u}) Y^*_{\ell m}(\hat{\boldsymbol{u}}) \, d\Omega(\hat{\boldsymbol{u}}) = 4\pi (-i)^\ell j_\ell (2\pi \|\boldsymbol{u}\|) \left(A^1 \cdot I^1\right)_{\ell m} .$$

- But not in practise since would require full sampling of the visibility function in $\mathbb{R}^3$.
- Instead use:
  - Standard Fourier transform approach for small patches.
  - w-projection (Cornwell *et al.* [3]) or faceting (Cornwell & Perley [4]) approaches for wide fields of view.
- We consider only the forward problem of simulating visibilities in the full-sky setting and do not consider the reverse problem of image reconstruction any further.

Outline

Why wavelets?

Fourier (1807)

Haar (1909)

Morlet and Grossman (1981)

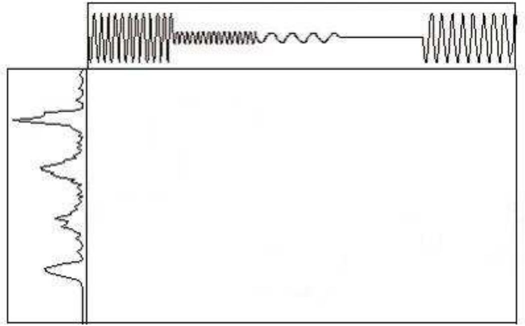

Figure: Fourier vs wavelet transform (image from `http://www.wavelet.org/tutorial/`)

Why wavelets?

Fourier (1807)

Haar (1909)

Morlet and Grossman (1981)

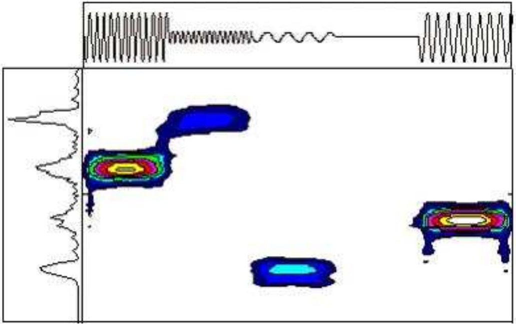

Figure: Fourier vs wavelet transform (image from http://www.wavelet.org/tutorial/)

Haar wavelets on the sphere

- Wavelets on the sphere
  - Continuous wavelets
    e.g. Antoine & Vandergheynst 1998 [1], Wiaux *et al.* 2005 [9]
  - Discrete/discretised wavelets
    e.g. Schroder & Sweldens 1995 [7], Barreio *et al.* 2000 [2], McEwen & Eyers 2008 [6], Starck *et al.* 2006 [8], Wiaux *et al.* 2008 [10]
- Define approximation spaces on the sphere $V_j \subset \mathrm{L}^2(\mathrm{S}^2)$
- Construct the nested hierarchy of approximation spaces

$$V_1 \subset V_2 \subset \cdots \subset V_J \subset \mathrm{L}^2(\mathrm{S}^2) ,$$

  where coarser (finer) approximation spaces correspond to a lower (higher) resolution level j.
- For each space V_j we define a basis with basis elements given by the *scaling functions* $\varphi_{j,k} \in V_j$, where the k index corresponds to a translation on the sphere.
- Define detail space W_j to be the orthogonal complement of V_j in V_{j+1}, *i.e.* $V_{j+1} = V_j \oplus W_j$.
- For each space W_j we define a basis with basis elements given by the *wavelets* $\psi_{j,k} \in W_j$.
- Expanding the hierarchy of approximation spaces:

$$V_J = V_1 \oplus \bigoplus_{j=1}^{J-1} W_j .$$

Haar wavelets on the sphere

- Wavelets on the sphere
  - Continuous wavelets
    e.g. Antoine & Vandergheynst 1998 [1], Wiaux *et al.* 2005 [9]
  - Discrete/discretised wavelets
    e.g. Schroder & Sweldens 1995 [7], Barreio *et al.* 2000 [2], McEwen & Eyers 2008 [6], Starck *et al.* 2006 [8], Wiaux *et al.* 2008 [10]
- Define approximation spaces on the sphere $V_j \subset L^2(S^2)$
- Construct the nested hierarchy of approximation spaces

$$V_1 \subset V_2 \subset \cdots \subset V_J \subset L^2(S^2) \,,$$

  where coarser (finer) approximation spaces correspond to a lower (higher) resolution level j.
- For each space V_j we define a basis with basis elements given by the *scaling functions* $\varphi_{j,k} \in V_j$, where the k index corresponds to a translation on the sphere.
- Define detail space W_j to be the orthogonal complement of V_j in V_{j+1}, *i.e.* $V_{j+1} = V_j \oplus W_j$.
- For each space W_j we define a basis with basis elements given by the *wavelets* $\psi_{j,k} \in W_j$.
- Expanding the hierarchy of approximation spaces:

$$V_J = V_1 \oplus \bigoplus_{j=1}^{J-1} W_j \,.$$

Haar wavelets on the sphere

- Wavelets on the sphere
  - Continuous wavelets
    e.g. Antoine & Vandergheynst 1998 [1], Wiaux *et al.* 2005 [9]
  - Discrete/discretised wavelets
    e.g. Schroder & Sweldens 1995 [7], Barreio *et al.* 2000 [2], McEwen & Eyers 2008 [6], Starck *et al.* 2006 [8], Wiaux *et al.* 2008 [10]
- Define approximation spaces on the sphere $V_j \subset \mathrm{L}^2(\mathrm{S}^2)$
- Construct the nested hierarchy of approximation spaces

$$V_1 \subset V_2 \subset \cdots \subset V_J \subset \mathrm{L}^2(\mathrm{S}^2) ,$$

  where coarser (finer) approximation spaces correspond to a lower (higher) resolution level j.
- For each space V_j we define a basis with basis elements given by the *scaling functions* $\varphi_{j,k} \in V_j$, where the k index corresponds to a translation on the sphere.
- Define detail space W_j to be the orthogonal complement of V_j in V_{j+1}, *i.e.* $V_{j+1} = V_j \oplus W_j$.
- For each space W_j we define a basis with basis elements given by the *wavelets* $\psi_{j,k} \in W_j$.
- Expanding the hierarchy of approximation spaces:

$$V_J = V_1 \oplus \bigoplus_{j=1}^{J-1} W_j .$$

Haar wavelets on the sphere

- Relate generic multiresolution decomposition to HEALPix pixelisation.
- Let V_j correspond to a HEALPix pixelised sphere with resolution parameter $N_{\rm side} = 2^{j-1}$.
- Define the scaling function $\varphi_{j,k}$ at level j to be constant for pixel k and zero elsewhere:

$$\varphi_{j,k}(\hat{s}) \equiv \begin{cases} 1/\sqrt{A_j} & \hat{s} \in P_{j,k} \\ 0 & \text{elsewhere} . \end{cases}$$

- Orthonormal basis for the wavelet space W_j given by the following wavelets:

$$\psi^0_{j,k}(\hat{s}) \equiv \left[\varphi_{j+1,k_0}(\hat{s}) - \varphi_{j+1,k_1}(\hat{s}) + \varphi_{j+1,k_2}(\hat{s}) - \varphi_{j+1,k_3}(\hat{s})\right]/2 ;$$
$$\psi^1_{j,k}(\hat{s}) \equiv \left[\varphi_{j+1,k_0}(\hat{s}) + \varphi_{j+1,k_1}(\hat{s}) - \varphi_{j+1,k_2}(\hat{s}) - \varphi_{j+1,k_3}(\hat{s})\right]/2 ;$$
$$\psi^2_{j,k}(\hat{s}) \equiv \left[\varphi_{j+1,k_0}(\hat{s}) - \varphi_{j+1,k_1}(\hat{s}) - \varphi_{j+1,k_2}(\hat{s}) + \varphi_{j+1,k_3}(\hat{s})\right]/2 .$$

Haar wavelets on the sphere

- Relate generic multiresolution decomposition to HEALPix pixelisation.
- Let V_j correspond to a HEALPix pixelised sphere with resolution parameter $N_{\rm side} = 2^{j-1}$.
- Define the scaling function $\varphi_{j,k}$ at level j to be constant for pixel k and zero elsewhere:

$$\varphi_{j,k}(\hat{\mathbf{s}}) \equiv \begin{cases} 1/\sqrt{A_j} & \hat{\mathbf{s}} \in P_{j,k} \\ 0 & \text{elsewhere} . \end{cases}$$

- Orthonormal basis for the wavelet space W_j given by the following wavelets:

$$\psi^0_{j,k}(\hat{\mathbf{s}}) \equiv \left[\varphi_{j+1,k_0}(\hat{\mathbf{s}}) - \varphi_{j+1,k_1}(\hat{\mathbf{s}}) + \varphi_{j+1,k_2}(\hat{\mathbf{s}}) - \varphi_{j+1,k_3}(\hat{\mathbf{s}})\right]/2 ;$$

$$\psi^1_{j,k}(\hat{\mathbf{s}}) \equiv \left[\varphi_{j+1,k_0}(\hat{\mathbf{s}}) + \varphi_{j+1,k_1}(\hat{\mathbf{s}}) - \varphi_{j+1,k_2}(\hat{\mathbf{s}}) - \varphi_{j+1,k_3}(\hat{\mathbf{s}})\right]/2 ;$$

$$\psi^2_{j,k}(\hat{\mathbf{s}}) \equiv \left[\varphi_{j+1,k_0}(\hat{\mathbf{s}}) - \varphi_{j+1,k_1}(\hat{\mathbf{s}}) - \varphi_{j+1,k_2}(\hat{\mathbf{s}}) + \varphi_{j+1,k_3}(\hat{\mathbf{s}})\right]/2 .$$

Haar wavelets on the sphere

- Relate generic multiresolution decomposition to HEALPix pixelisation.
- Let V_j correspond to a HEALPix pixelised sphere with resolution parameter $N_{\text{side}} = 2^{j-1}$.
- Define the scaling function $\varphi_{j,k}$ at level j to be constant for pixel k and zero elsewhere:

$$\varphi_{j,k}(\hat{\mathbf{s}}) \equiv \begin{cases} 1/\sqrt{A_j} & \hat{\mathbf{s}} \in P_{j,k} \\ 0 & \text{elsewhere} . \end{cases}$$

- Orthonormal basis for the wavelet space W_j given by the following wavelets:

$$\psi^0_{j,k}(\hat{\mathbf{s}}) \equiv \left[\varphi_{j+1,k_0}(\hat{\mathbf{s}}) - \varphi_{j+1,k_1}(\hat{\mathbf{s}}) + \varphi_{j+1,k_2}(\hat{\mathbf{s}}) - \varphi_{j+1,k_3}(\hat{\mathbf{s}})\right]/2 ;$$
$$\psi^1_{j,k}(\hat{\mathbf{s}}) \equiv \left[\varphi_{j+1,k_0}(\hat{\mathbf{s}}) + \varphi_{j+1,k_1}(\hat{\mathbf{s}}) - \varphi_{j+1,k_2}(\hat{\mathbf{s}}) - \varphi_{j+1,k_3}(\hat{\mathbf{s}})\right]/2 ;$$
$$\psi^2_{j,k}(\hat{\mathbf{s}}) \equiv \left[\varphi_{j+1,k_0}(\hat{\mathbf{s}}) - \varphi_{j+1,k_1}(\hat{\mathbf{s}}) - \varphi_{j+1,k_2}(\hat{\mathbf{s}}) + \varphi_{j+1,k_3}(\hat{\mathbf{s}})\right]/2 .$$

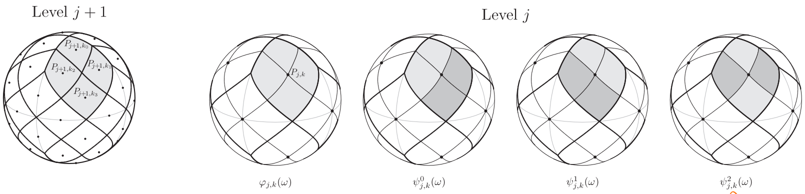

Figure: Haar scaling function $\varphi_{j,k}(\hat{\mathbf{s}})$ and wavelets $\psi^m_{j,k}(\hat{\mathbf{s}})$

Haar wavelets on the sphere

- Multiresolution decomposition of a function defined on a HEALPix data-sphere at resolution J, *i.e.* $f_J \in V_J$ proceeds as follows.

- Approximation coefficients at the coarser level j are given by the projection of f_{j+1} onto the scaling functions $\varphi_{j,k}$:

$$\lambda_{j,k} = \int_{S^2} f_{j+1}(\hat{\mathbf{s}})\ \varphi_{j,k}(\hat{\mathbf{s}})\ \ \mathrm{d}\Omega(\hat{\mathbf{s}})\ .$$

- Detail coefficients at level j are given by the projection of f_{j+1} onto the wavelets $\psi^m_{j,k}$:

$$\gamma^m_{j,k} = \int_{S^2} f_{j+1}(\hat{\mathbf{s}})\ \psi^m_{j,k}(\hat{\mathbf{s}})\ \ \mathrm{d}\Omega(\hat{\mathbf{s}})\ .$$

- The function $f_J \in V_J$ may then be synthesised from its approximation and detail coefficients:

$$f_J(\hat{\mathbf{s}}) = \sum_{k=0}^{N_{J_0}-1} \lambda_{J_0 k}\varphi_{J_0 k}(\hat{\mathbf{s}}) + \sum_{j=J_0}^{J-1}\sum_{k=0}^{N_j-1}\sum_{m=0}^{2} \gamma^m_{j,k}\psi^m_{j,k}(\hat{\mathbf{s}})\ .$$

ÉCOLE POLYTECHNIQUE FÉDÉRALE DE LAUSANNE

Haar wavelets on the sphere

- Multiresolution decomposition of a function defined on a HEALPix data-sphere at resolution J, *i.e.* $f_J \in V_J$ proceeds as follows.
- Approximation coefficients at the coarser level j are given by the projection of f_{j+1} onto the scaling functions $\varphi_{j,k}$:

$$\lambda_{j,k} = \int_{S^2} f_{j+1}(\hat{\mathbf{s}})\ \varphi_{j,k}(\hat{\mathbf{s}})\ \mathrm{d}\Omega(\hat{\mathbf{s}})\ .$$

- Detail coefficients at level j are given by the projection of f_{j+1} onto the wavelets $\psi^m_{j,k}$:

$$\gamma^m_{j,k} = \int_{S^2} f_{j+1}(\hat{\mathbf{s}})\ \psi^m_{j,k}(\hat{\mathbf{s}})\ \mathrm{d}\Omega(\hat{\mathbf{s}})\ .$$

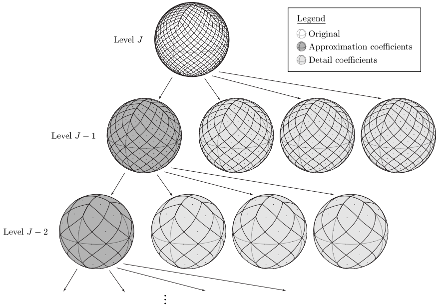

Figure: Haar multiresolution decomposition

- The function $f_J \in V_J$ may then be synthesised from its approximation and detail coefficients:

$$f_J(\hat{\mathbf{s}}) = \sum_{k=0}^{N_{J_0}-1} \lambda_{J_0 k}\varphi_{J_0 k}(\hat{\mathbf{s}}) + \sum_{j=J_0}^{J-1}\sum_{k=0}^{N_j-1}\sum_{m=0}^{2} \gamma^m_{j,k}\psi^m_{j,k}(\hat{\mathbf{s}})\ .$$

Haar wavelets on the sphere

- Multiresolution decomposition of a function defined on a `HEALPix` data-sphere at resolution J, *i.e.* $f_J \in V_J$ proceeds as follows.
- Approximation coefficients at the coarser level j are given by the projection of f_{j+1} onto the scaling functions $\varphi_{j,k}$:

$$\lambda_{j,k} = \int_{S^2} f_{j+1}(\hat{\mathbf{s}})\ \varphi_{j,k}(\hat{\mathbf{s}})\ \mathrm{d}\Omega(\hat{\mathbf{s}})\ .$$

- Detail coefficients at level j are given by the projection of f_{j+1} onto the wavelets $\psi^m_{j,k}$:

$$\gamma^m_{j,k} = \int_{S^2} f_{j+1}(\hat{\mathbf{s}})\ \psi^m_{j,k}(\hat{\mathbf{s}})\ \mathrm{d}\Omega(\hat{\mathbf{s}})\ .$$

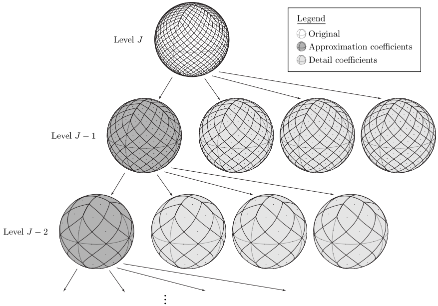

Figure: Haar multiresolution decomposition

- The function $f_J \in V_J$ may then be synthesised from its approximation and detail coefficients:

$$f_J(\hat{\mathbf{s}}) = \sum_{k=0}^{N_{J_0}-1} \lambda_{J_0 k}\varphi_{J_0 k}(\hat{\mathbf{s}}) + \sum_{j=J_0}^{J-1}\sum_{k=0}^{N_j-1}\sum_{m=0}^{2} \gamma^m_{j,k}\psi^m_{j,k}(\hat{\mathbf{s}})\ .$$

Outline

SHW visibility representation

- Representing the beam-modulated intensity and the plane wave in an orthogonal wavelet basis on the sphere, with wavelets $\Psi_j(\hat{s}) \in L^2(S^2, d\Omega)$:

$$(A^l \cdot I^l)(\hat{s}^l) = \sum_j (A^l \cdot I^l)_j \Psi_j(\hat{s}^l) \ ;$$

$$e^{i2\pi \boldsymbol{u} \cdot \hat{s}^l} = \sum_k E_k(\boldsymbol{u}) \Psi_k(\hat{s}^l) \ .$$

- Wavelet coefficients are given by the projection onto the wavelet basis functions:

$$(A^l \cdot I^l)_j = \int_{S^2} (A^l \cdot I^l)(\hat{s}^l) \Psi_j^*(\hat{s}^l) \, d\Omega(\hat{s}^l) \ ;$$

$$E_k(\boldsymbol{u}) = \int_{S^2} e^{i2\pi \boldsymbol{u} \cdot \hat{s}^l} \Psi_k^*(\hat{s}^l) \, d\Omega(\hat{s}^l) \ .$$

- Substituting these expansions into the visibility integral, and noting the orthogonality of the wavelet basis, we find:

SHW representation of visibility

$$\mathcal{V}(\boldsymbol{u}) = \sum_j (A^l \cdot I^l)_j E_j^*(\boldsymbol{u})$$

SHW visibility representation

- Representing the beam-modulated intensity and the plane wave in an orthogonal wavelet basis on the sphere, with wavelets $\Psi_j(\hat{\boldsymbol{s}}) \in \mathrm{L}^2(\mathrm{S}^2,\, \mathrm{d}\Omega)$:

$$\left(A^{\mathrm{l}} \cdot I^{\mathrm{l}}\right)(\hat{\boldsymbol{s}}^{\mathrm{l}}) = \sum_j \left(A^{\mathrm{l}} \cdot I^{\mathrm{l}}\right)_j \Psi_j(\hat{\boldsymbol{s}}^{\mathrm{l}}) \;;$$

$$\mathrm{e}^{\mathrm{i}2\pi \boldsymbol{u}\cdot\hat{\boldsymbol{s}}^{\mathrm{l}}} = \sum_k E_k(\boldsymbol{u}) \Psi_k(\hat{\boldsymbol{s}}^{\mathrm{l}}) \;.$$

- Wavelet coefficients are given by the projection onto the wavelet basis functions:

$$\left(A^{\mathrm{l}} \cdot I^{\mathrm{l}}\right)_j = \int_{\mathrm{S}^2} \left(A^{\mathrm{l}} \cdot I^{\mathrm{l}}\right)(\hat{\boldsymbol{s}}^{\mathrm{l}}) \Psi_j^*(\hat{\boldsymbol{s}}^{\mathrm{l}})\, \mathrm{d}\Omega(\hat{\boldsymbol{s}}^{\mathrm{l}}) \;;$$

$$E_k(\boldsymbol{u}) = \int_{\mathrm{S}^2} \mathrm{e}^{\mathrm{i}2\pi \boldsymbol{u}\cdot\hat{\boldsymbol{s}}^{\mathrm{l}}} \Psi_k^*(\hat{\boldsymbol{s}}^{\mathrm{l}})\, \mathrm{d}\Omega(\hat{\boldsymbol{s}}^{\mathrm{l}}) \;.$$

- Substituting these expansions into the visibility integral, and noting the orthogonality of the wavelet basis, we find:

SHW representation of visibility

$$\mathcal{V}(\boldsymbol{u}) = \sum_j \left(A^{\mathrm{l}} \cdot I^{\mathrm{l}}\right)_j E_j^*(\boldsymbol{u})$$

Fast wavelet algorithms

- Computing visibilities from the SHW representation naively is no more efficient than the spherical harmonic representation.
- However, $(A^l \cdot I^l)$ is sparse in the wavelet basis.
- By exploiting sparsity many wavelet coefficients can be ignored, reducing the computational cost of the calculation significantly.
- Consider a number of algorithms to determine wavelet coefficients that contain non-negligible information content and compute visibilities using only these coefficients:
  - Hard thresholding
  - Annealing thresholding strategies to favour coarser levels
    $\longrightarrow$ quadratic annealing most effective
- Naive complexity of computing visibility for given $\boldsymbol{u}$ is $\mathcal{O}(J)$, where J is the number of basis functions used in the representation.
  - For the spherical harmonic basis $\mathcal{O}(J) \sim \mathcal{O}({\ell_{\max}}^2) \sim \mathcal{O}(u_{\max}^2)$
  - For the SHW basis typically $\mathcal{O}(J) \sim \mathcal{O}(u_{\max}^n)$ for $n \lesssim 1$

Fast wavelet algorithms

- Computing visibilities from the SHW representation naively is no more efficient than the spherical harmonic representation.
- However, $(A^{\mathrm{l}} \cdot I^{\mathrm{l}})$ is sparse in the wavelet basis.
- By exploiting sparsity many wavelet coefficients can be ignored, reducing the computational cost of the calculation significantly.
- Consider a number of algorithms to determine wavelet coefficients that contain non-negligible information content and compute visibilities using only these coefficients:
  - Hard thresholding
  - Annealing thresholding strategies to favour coarser levels
    $\longrightarrow$ quadratic annealing most effective
- Naive complexity of computing visibility for given $\boldsymbol{u}$ is $\mathcal{O}(J)$, where J is the number of basis functions used in the representation.
  - For the spherical harmonic basis $\mathcal{O}(J) \sim \mathcal{O}({\ell_{\max}}^2) \sim \mathcal{O}(u_{\max}^2)$
  - For the SHW basis typically $\mathcal{O}(J) \sim \mathcal{O}(u_{\max}^n)$ for $n \lesssim 1$

Fast wavelet algorithms

- Computing visibilities from the SHW representation naively is no more efficient than the spherical harmonic representation.
- However, $(A^{l} \cdot I^{l})$ is sparse in the wavelet basis.
- By exploiting sparsity many wavelet coefficients can be ignored, reducing the computational cost of the calculation significantly.
- Consider a number of algorithms to determine wavelet coefficients that contain non-negligible information content and compute visibilities using only these coefficients:
  - Hard thresholding
  - Annealing thresholding strategies to favour coarser levels $\longrightarrow$ quadratic annealing most effective
- Naive complexity of computing visibility for given $\boldsymbol{u}$ is $\mathcal{O}(J)$, where J is the number of basis functions used in the representation.
  - For the spherical harmonic basis $\mathcal{O}(J) \sim \mathcal{O}({\ell_{\text{max}}}^2) \sim \mathcal{O}(u_{\text{max}}^2)$
  - For the SHW basis typically $\mathcal{O}(J) \sim \mathcal{O}(u_{\text{max}}^n)$ for $n \lesssim 1$

ÉCOLE POLYTECHNIQUE FÉDÉRALE DE LAUSANNE

Fast wavelet algorithms

- Computing visibilities from the SHW representation naively is no more efficient than the spherical harmonic representation.
- However, $(A^{\mathrm{l}} \cdot I^{\mathrm{l}})$ is sparse in the wavelet basis.
- By exploiting sparsity many wavelet coefficients can be ignored, reducing the computational cost of the calculation significantly.
- Consider a number of algorithms to determine wavelet coefficients that contain non-negligible information content and compute visibilities using only these coefficients:
  - Hard thresholding
  - Annealing thresholding strategies to favour coarser levels
    $\longrightarrow$ quadratic annealing most effective
- Naive complexity of computing visibility for given $\boldsymbol{u}$ is $\mathcal{O}(J)$, where J is the number of basis functions used in the representation.
  - For the spherical harmonic basis $\mathcal{O}(J) \sim \mathcal{O}({\ell_{\mathrm{max}}}^2) \sim \mathcal{O}(u_{\mathrm{max}}^2)$
  - For the SHW basis typically $\mathcal{O}(J) \sim \mathcal{O}(u_{\mathrm{max}}^n)$ for $n \lesssim 1$

Outline

Low-resolution simulations

- Perform low-resolution simulations of mock observations of synchrotron emission (use synchrotron foreground map recovered from WMAP observations)
- Low-resolution simulations: baseline limit of $u_{\max} = 30$; reconstruct 20×20 image (corresponds to $\sim 20^\circ$ square patch).
- Rotate to local coordinates then compute visibilities for complete uv coverage, including full-sky contributions.
- Assume Gaussian beam of $\mathrm{FWHM}_\mathrm{b} \simeq 18^\circ$.

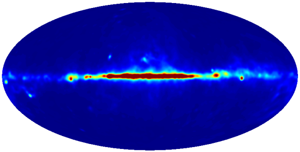

(a) Synchrotron map (global coord.)

Figure: Synchrotron emission and beam maps

Low-resolution simulations

- Perform low-resolution simulations of mock observations of synchrotron emission (use synchrotron foreground map recovered from WMAP observations)
- Low-resolution simulations: baseline limit of $u_{\max} = 30$; reconstruct 20×20 image (corresponds to $\sim 20^\circ$ square patch).
- Rotate to local coordinates then compute visibilities for complete uv coverage, including full-sky contributions.
- Assume Gaussian beam of $\mathrm{FWHM_b} \simeq 18^\circ$.

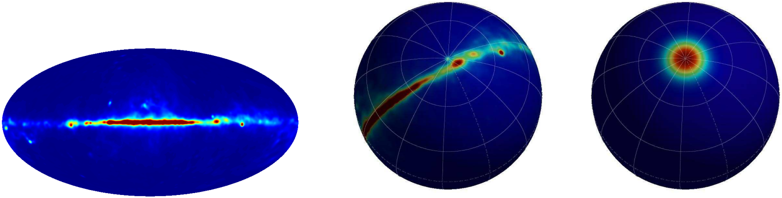

(a) Synchrotron map (global coord.) (b) Synchrotron map (local coord.) (c) Gaussian beam (local coord.)

Figure: Synchrotron emission and beam maps

Low-resolution simulations

- Simulate visibilities using all methods and reconstruct images simply using Fourier transform.
- Reconstructed images and tangent plane image all in close agreement
(expect some difference since full-sky contributions included when simulating visibilities but tangent plane approximation assumed to recover images).

Low-resolution simulations

- Simulate visibilities using all methods and reconstruct images simply using Fourier transform.
- Reconstructed images and tangent plane image all in close agreement
  (expect some difference since full-sky contributions included when simulating visibilities but tangent plane approximation assumed to recover images).

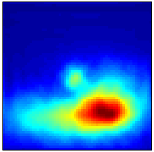

(a) Tangent plane image

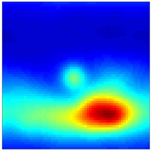

(b) Direct quadrature

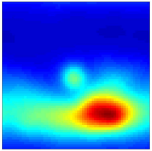

(c) Spherical harmonics

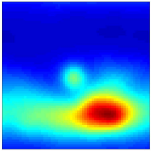

(d) Naive SHW

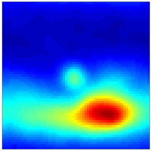

(e) Thresholded SHW (constant threshold)

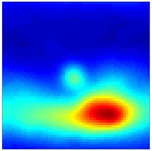

(f) Thresholded SHW (annealing strategy)

Figure: Original and reconstructed images.

Low-resolution simulations

- Compare performance of the methods for simulating interferometric observations in the full-sky setting (on laptop with 2.2GHz Intel Core 2 Duo processor and 2GB of memory).

Method	Complexity $\mathcal{O}(u_{\max}^n)$	Coefficients retained	Execution time
Direct quadrature	$n = 2$	100.00%	207.6s
Spherical harmonic	$n = 2$	100.00%	263.7s
Naive SHW	$n = 2$	100.00%	238.9s
Fast SHW (constant threshold)	$n \lesssim 1$	0.70%	75.8s
Fast SHW (annealing strategy)	$n \lesssim 1$	0.35%	73.0s

- Typically less than 1% of SHW coefficients required to represent the information content of the beam-modulated intensity map accurately.
- The already slow performance of the quadrature and spherical harmonic techniques and their poor scaling render these methods computationally infeasible for high-resolution problems.
- Fast SHW methods have much better scaling properties and are already considerably faster at this low-resolution, rendering realistic high-resolution simulations feasible.

Low-resolution simulations

- Compare performance of the methods for simulating interferometric observations in the full-sky setting (on laptop with 2.2GHz Intel Core 2 Duo processor and 2GB of memory).

Method	Complexity $\mathcal{O}(u_{\max}^n)$	Coefficients retained	Execution time
Direct quadrature	$n = 2$	100.00%	207.6s
Spherical harmonic	$n = 2$	100.00%	263.7s
Naive SHW	$n = 2$	100.00%	238.9s
Fast SHW (constant threshold)	$n \lesssim 1$	0.70%	75.8s
Fast SHW (annealing strategy)	$n \lesssim 1$	0.35%	73.0s

- Typically less than 1% of SHW coefficients required to represent the information content of the beam-modulated intensity map accurately.
- The already slow performance of the quadrature and spherical harmonic techniques and their poor scaling render these methods computationally infeasible for high-resolution problems.
- Fast SHW methods have much better scaling properties and are already considerably faster at this low-resolution, rendering realistic high-resolution simulations feasible.

High-resolution simulations

- Illustrate fast SHW simulations on higher resolution simulation of 94GHz FDS map of predicted submillimeter and microwave emission of diffuse interstellar Galactic dust [5].
- High-resolution simulations: baseline limit of $u_{\max} = 100$; reconstruct 20×20 image (corresponds to $\sim 6^\circ$ square patch).
- Assume Gaussian beam of $\mathrm{FWHM_b} \simeq 3^\circ$.

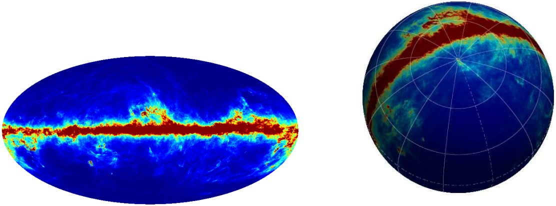

(a) Global coord. (b) Local coord.

Figure: Full-sky 94GHz FDS map of predicted emission of diffuse interstellar Galactic dust.

High-resolution simulations

- Original and reconstructed images in close agreement.
  Expect some difference since:
  - Full-sky contributions incorporated when simulating visibilities, however flat-patch approximation is assumed when synthesising the image
  - Fast SHW method introduces small error by discarding wavelet coefficients with minimal information
- Execution time of 290s (estimate $\sim$3000s for spherical harmonic method).
- Fast SHW algorithm therefore essential to compute full-sky interferometric contributions in realistic high-resolution simulations.
- Fast SHW algorithm also highly parallelisable.

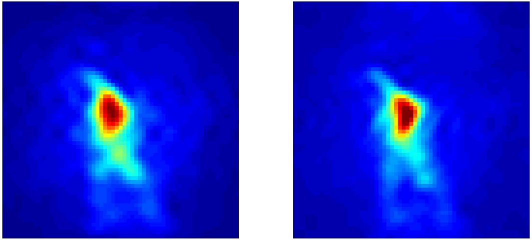

(a) Tangent plane image   (b) Fast SHW simulated image

Figure: Original and reconstructed images.

High-resolution simulations

- Original and reconstructed images in close agreement.
  Expect some difference since:
  - Full-sky contributions incorporated when simulating visibilities, however flat-patch approximation is assumed when synthesising the image
  - Fast SHW method introduces small error by discarding wavelet coefficients with minimal information
- Execution time of 290s (estimate $\sim$3000s for spherical harmonic method).
- Fast SHW algorithm therefore essential to compute full-sky interferometric contributions in realistic high-resolution simulations.
- Fast SHW algorithm also highly parallelisable.

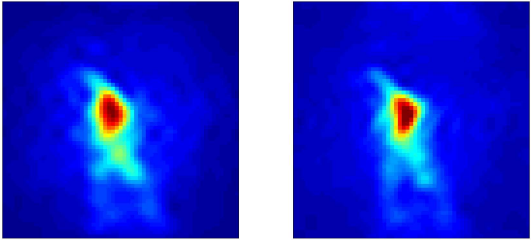

(a) Tangent plane image (b) Fast SHW simulated image

Figure: Original and reconstructed images.

Outline

Summary & future work

- Derived spherical harmonic and SHW representation of visibility integral, including full-sky contributions.
- Developed fast SHW algorithms to render full-sky interferometric simulations feasible for realistic, high-resolution settings.
- Demonstrated and verified algorithms on simulated observations.

- Future work:
  - More realistic high-resolution simulations (incomplete, realistic uvw coverage; time varying beams; parallelise implementation)
  - Study impact of ignoring full-sky effects
  - Incorporate wide field-of-view contributions when reconstructing images

Summary & future work

- Derived spherical harmonic and SHW representation of visibility integral, including full-sky contributions.
- Developed fast SHW algorithms to render full-sky interferometric simulations feasible for realistic, high-resolution settings.
- Demonstrated and verified algorithms on simulated observations.

- Future work:
  - More realistic high-resolution simulations
    (incomplete, realistic uvw coverage; time varying beams; parallelise implementation)
  - Study impact of ignoring full-sky effects
  - Incorporate wide field-of-view contributions when reconstructing images

References

[1] J.-P. Antoine and P. Vandergheynst.
Wavelets on the n-sphere and related manifolds.
J. Math. Phys., 39(8):3987–4008, 1998.

[2] R. B. Barreiro, M. P. Hobson, A. N. Lasenby, A. J. Banday, K. M. Górski, and G. Hinshaw.
Testing the Gaussianity of the COBE-DMR data with spherical wavelets.
Mon. Not. Roy. Astron. Soc., 318:475–481, 2000.

[3] T. J. Cornwell, K. Golap, and S. Bhatnagar.
Wide Field Imaging: Fourier and Fresnel.
In N. Kassim, M. Perez, W. Junor, and P. Henning, editors, *Astronomical Data Analysis Software and Systems XIV*, volume 345 of *Astronomical Society of the Pacific Conference Series*, pages 350–+, December 2005.

[4] T. J. Cornwell and R. A. Perley.
Radio-interferometric imaging of very large fields - The problem of non-coplanar arrays.
Astron. & Astrophys., 261:353–364, July 1992.

[5] D. P. Finkbeiner, M. Davis, and D. J. Schlegel.
Extrapolation of Galactic Dust Emission at 100 Microns to Cosmic Microwave Background Radiation Frequencies Using FIRAS.
Astrophys. J., 524:867–886, October 1999.

[6] J. D. McEwen and A. M. M. Scaife.
Simulating full-sky interferometric observations.
Mon. Not. Roy. Astron. Soc., 389(3):1163–1178, 2008.

[7] P. Schröder and W. Sweldens.
Spherical wavelets: efficiently representing functions on the sphere.
In *Computer Graphics Proceedings (SIGGRAPH '95)*, pages 161–172, 1995.

[8] J.-L. Starck, Y. Moudden, P. Abrial, and M. Nguyen.
Wavelets, ridgelets and curvelets on the sphere.
Astron. & Astrophys., 446:1191–1204, February 2006.

[9] Y. Wiaux, L. Jacques, and P. Vandergheynst.
Correspondence principle between spherical and Euclidean wavelets.
Astrophys. J., 632:15–28, 2005.

[10] Y. Wiaux, J. D. McEwen, P. Vandergheynst, and O. Blanc.
Exact reconstruction with directional wavelets on the sphere.
Mon. Not. Roy. Astron. Soc., 388(2):770–788, 2008.